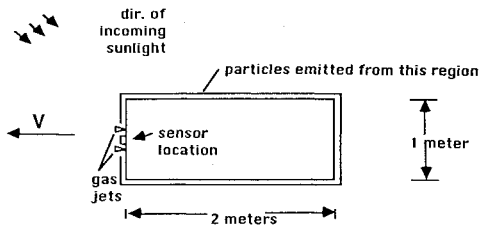

Fig. 1 Spacecraft model.

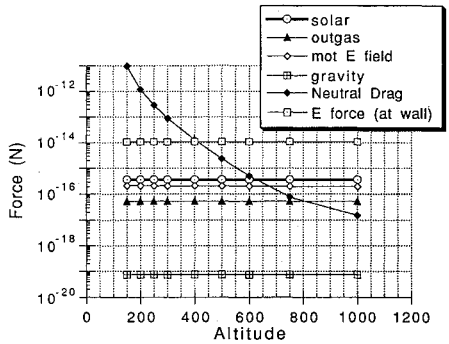

Fig. 2 Force on a 5-μ particle vs altitude (km).

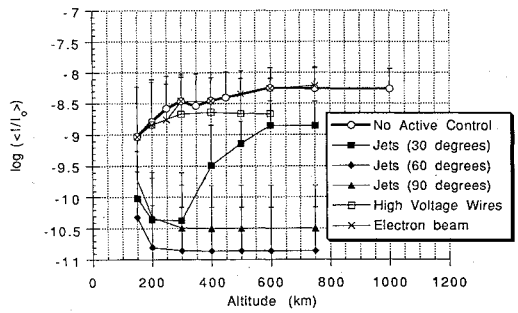

Fig. 3 Intensity plot (2-D) comparing all control methods.

dielectric breakdown strength. This is done to get an upper bound on the effectiveness of this method. In both cases, the spacecraft surface potential is assumed to be maintained by a plasma contactor in the back of the spacecraft.

III. Results

Simulations were performed for two and three dimensions, and over a range of equatorial LEOs with altitudes from 150 to 1000 km. The quantity of interest from the viewpoint of the sensor is the noise or scattered signal associated with the presence of the particles. The intensity of the scattered sunlight from the particles is determined using Mie scattering theory for particles much larger than the wavelength, so that the calculation is valid for visible light and for short-wavelength infrared radiation.[4] The scattered intensity normalized by the intensity of the incident radiation is proportional to the square of the ratio of particle radius to particle distance from the sensor. The total scattered intensity is determined as the sum of the scattered intensities of the particles.

For each altitude, the normalized scattered intensity is averaged over the first 10 s of each simulation. These intensity averages are shown in Fig. 3 (2-D case) and in Fig. 4 (3-D case). The error bars included in the plots indicate the standard deviation of the intensity average for each point.

The gasdynamic forces are seen clearly to be the superior method of affecting the particles. In the 2-D case, there is improvement of one to three orders of magnitude in the average normalized scattered intensity. The 3-D improvements are far less dramatic, due to the fact that the particles may travel between gas jets to reach the sensor view, thus avoiding the strongest areas of control. Four additional

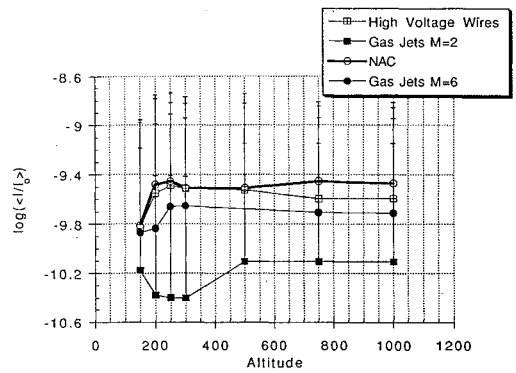

Fig. 4 Intensity plot (3-D) comparing effectiveness of control methods.

gas jets were added in this case, but that was insufficient to yield comparable results to the 2-D case. This implies that they would be quite effective if particulates are generated from a specific location on the spacecraft.

In general it is observed to be the case that for this range of particle sizes, the control methods that rely on electromagnetic forces are significantly less effective than the gasdynamic ones. If the particles of concern, however, had a higher charge/mass ratio, electromagnetic methods would have been more effective than they were here.

Acknowledgment

This work was supported by funds from The Johns Hopkins University Applied Physics Laboratory.

References

[1]Smith, B. A., "JPL Monitoring Satellite Systems," *Aviation Week and Space Technology*, Oct. 5, 1992, p. 24.

[2]Rawlins, W. T., and Green B. D., "Spectral Signatures of Micron Sized Particles in the Shuttle Optical Environment," *Applied Optics*, Vol. 26, 1987, p. 3052.

[3]Dettleff, G., "Plume Flow and Plume Impingement in Space Technology," *Progress in Aerospace Science*, Vol. 28, 1991, pp. 1–71.

[4]van de Hulst, H. C., *Light Scattering by Small Particles*, Academic Press, New York, 1981, pp. 200–206.

Laser Velocimetry Seed-Particle Behavior in Shear Layers at Mach 12

J. D. Schmisseur* and M. S. Maurice†
Wright Laboratory,
Wright-Patterson Air Force Base, Ohio 45433-7005

Introduction

ALTHOUGH laser velocimetry (LV) methods have been employed since the 1960s, the LV data base for hypersonic flows is extremely limited. That is primarily because frequency-domain and counter processors with the ability to efficiently examine the high-frequency signal bursts associated with hypersonic particles have only recently become available. Another factor contributing to the lack of hypersonic data is poor seed particle response characteristics. The considerable momentum possessed by particles at hypersonic velocities prevents them from accurately tracking the fluid streamlines. Because LV systems measure the velocity of the

Received Feb. 18, 1994; revision received Oct. 17, 1994; accepted for publication Oct. 28, 1994. This paper is declared a work of the U.S. Government and is not subject to copyright protection in the United States.

*Aerospace Engineer, Aeromechanics Division, Flight Dynamics Directorate. Member AIAA.

†Mechanical Engineer, Aeromechanics Division, Flight Dynamics Directorate. Senior Member AIAA.

seed particles and not the gas velocity, biased data can result. Thus, although the technology for LV measurements in the hypersonic regime is now available, an assessment of the physical validity of the resulting data is appropriate. Notable work of previous investigators is reviewed in Ref. 1.

In order to examine seed particle behavior in a Mach 12 flowfield, LV measurements were made in the Aeromechanics Division Twenty-Inch Hypersonic Wind Tunnel. Data were collected in the shear layer generated by the nozzle wall at the nozzle exit plane. Two diameters of alumina, nominally 0.3 and 1.0 μm, were used as seed material to investigate the particle response characteristics.

Experimental Setup

Test Facility and Conditions

The Twenty Inch Hypersonic Wind Tunnel is an intermittent blowdown facility operating on high-pressure air (20.7 MPa) and exhausting into a vacuum sphere. The tunnel has a contoured, axisymmetric nozzle, 3.05 m in length, with a 0.508 m (20-in.) diameter at the exit plane where the flow enters the test cabin as a free jet. Calibration of the test-section flow has shown that the Mach number is 12.31 on the tunnel centerline, 2.54 cm downstream of the nozzle exit.[2] Optical access is provided by 35.6-cm-diam schlieren-quality windows on either side of the test cabin.

For the current experiment, the reservoir air was heated to 1056 K at a pressure of 5.5 MPa. The freestream velocity and unit Reynolds number in the test section, calculated using the reservoir conditions and the calibrated Mach number and corrected for caloric imperfections,[3] are 1466 m/s and 1.7×10^6 m^{-1}, respectively. Keyes's viscosity law[4] has been used to calculate the Reynolds number.

LV Configuration

The LV system was configured to measure the axial component of the tunnel velocity from forward scattering of the 514.5-nm line from an argon ion laser. The fringe spacing was 20.8 μm, and the probe volume was 0.58 mm in diameter and 94.4 mm long. The collected light from the test section was focused onto a 1-mm-diam fiber-optic cable, which carried the collected light to a color separator. The magnification of the collection system was 0.5, and the angle of the collection optical axis with respect to the transmission optical axis was 28.8 deg. Hence, the effective probe-volume length was 4.1 mm. Both transmission and collection optics were mounted on independent machinist-style traverses, which allowed the optics to be moved in three dimensions.

The electronic signal output by the photomultiplier tube was amplified and then recorded and analyzed by a fast-Fourier-transform-based signal processor. Data at each coordinate were collected until 1000 valid bursts were realized or until the maximum collection period of 60 s expired. Statistical analysis of each data set was then performed on a mini-VAX computer.

Seed Materials

Response characteristics were examined for two sizes of alumina. As quoted by the manufacturer, the nominal particle diameters were 0.3 and 1.0 μm, respectively, with a density of 3700 kg/m^3. The seed was introduced into the tunnel between the reservoir and the nozzle via a fluidized-bed seeder designed for the experiment. The alumina seed material was chosen because it was readily available in the laboratory. Since particle size distributions are required for analysis of the particle dynamics, the solid seed material of known size was used instead of a less dense wet seed material. Qualitatively, the alumina seed appeared to have good scattering characteristics, as evidenced by high data collection rates, on the order of several hundred hertz.

CFD Solution

In order to numerically estimate the seed particle behavior through the nozzle, a computational solution for the flowfield is required. The solution used for this analysis incorporates three discrete sequential calculations, each optimized for a specific flow regime in the nozzle.[5] For the subsonic and transonic flow in the throat region, a full Navier-Stokes solution was generated using the PARC code. In the supersonic nozzle expansion a parabolized Navier-Stokes scheme, SCRINT-X, was used. Both the PARC and SCRINT-X solutions employed the same k-ε turbulence model and allowed for equilibrium real-gas effects. Finally, in the test section, the free jet was calculated using SPF (standard plume flowfield), an Euler (inviscid) code. Reference 5 contains a description of the computational solution as well as references for the various calculation schemes.

Results

Measured mean-velocity profiles for the shear layer generated by the nozzle boundary layer as it enters the test section are shown in Fig. 1 for both seed sizes. The computational prediction is also plotted for comparison. Note that the profiles approach the same freestream velocity but have distinctly different shapes within the shear layer.

In an attempt to understand the factors contributing to the individual velocity profiles in the shear layer, the trajectories of seed particles with various diameters were estimated by tracking numerical models of the particles through the existing computational solution. The computed flow conditions at each point in the particle path were used to determine the local particle dynamics. The technique is described in detail in Ref. 6.

The computed nozzle streamlines and the numerically estimated particle trajectories for 0.3-, 1.0-, and 5.0-μm particles are plotted in Fig. 2. From visual inspection, the estimated trajectories show that particles do not follow the fluid streamlines. An example of this is near the nozzle wall, where the particle trajectories indicate that particles from the external, inviscid region are entering the boundary-layer region. This influx of high-velocity particles into the lower-velocity boundary layer explains the measured velocity profiles, which are fuller than that predicted by the computational solution (Fig. 1).

Corrected Velocity Profiles

Using the nominal particle diameters quoted by the manufacturer, the velocities of seed particles in the shear layer were estimated numerically and the resulting estimated velocity lag bias used to correct the experimental data. For the nominal 0.3-μm alumina, the corrected profile is still fuller than the computational prediction. This undercorrection is explained by the raw histograms of the velocity measurements, presented in Ref. 1. In these histograms the 0.3-μm data show bimodal distributions, which are indicative of polydisperse particle sizes. The presence of more than one seed diameter in the 0.3-μm seed material is verified by electron microscope photographs.[1] Hence, the velocity correction based on estimating the lag bias of a monodisperse seed material will not accurately represent the actual measured bias. A more accurate assessment of the size distribution is required for improved quantitative correction of the data.

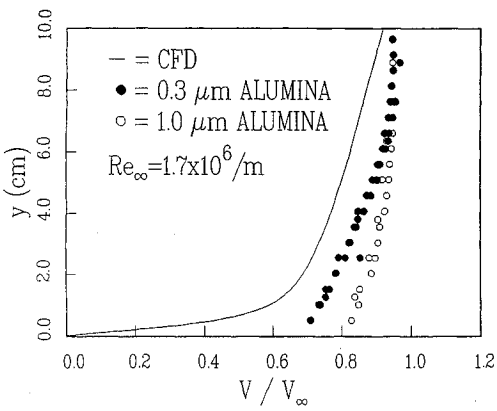

Fig. 1 Measured mean-velocity profiles at the nozzle exit. Velocities are normalized by the freestream velocity; y denotes the distance from the nozzle wall toward the nozzle centerline.

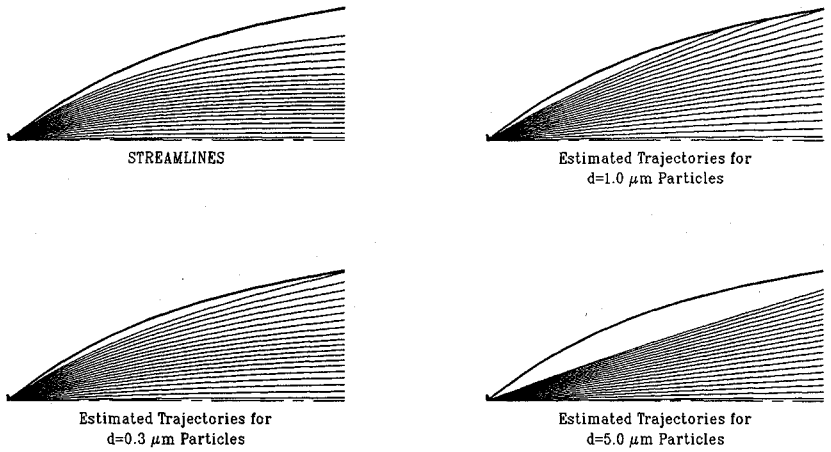

Fig. 2 Computed streamlines and particle trajectories through the nozzle.

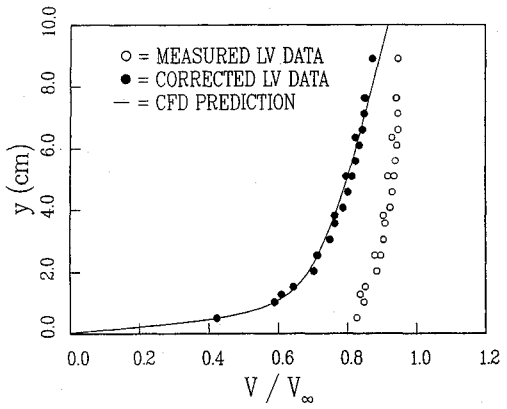

Fig. 3 Original and corrected velocity profiles for 1.0-μm alumina particles.

The raw and corrected velocity profiles for the 1.0-μm alumina are shown in Fig. 3. The velocity profile from the computational solution is plotted for comparison. In contrast to the 0.3-μm profile, the 1.0-μm-seed corrected profile shape agrees extremely well with the CFD prediction, because of the reasonably accurate modeling of the particle size. The excellent agreement between the corrected measurements and the computational prediction show that the particle velocity lag bias may be accounted for in hypersonic flows with very weak gradients.

Conclusions

The feasibility of LV measurements at Mach 12 has been examined for the Aeromechanics Division Twenty-Inch Hypersonic Wind Tunnel. Velocity measurements using nominally 0.3- and 1.0-μm alumina seed particles reveal the following: 1) seed particles of various diameters have different response characteristics, which result in particle-size-dependent velocity profiles, even within the relatively mild flow gradients encountered within the shear layer; 2) corrected velocity profiles for the nominally 1.0-μm alumina agree extremely well with the CFD prediction. Velocity profiles for the nominally 0.3-μm particles do not show as good agreement, because of contamination by at least one additional particle size. Although the current study has shown that accurate shear-layer profiles may be obtained by correcting experimental data with a numerically estimated velocity lag, the poor particle response to even the mildest gradients in the flowfield indicates that LV measurements using alumina seed larger than 0.3 μm in diameter are not a suitable diagnostic for the Mach 12 facility.

References

[1]Schmisseur, J. D., and Maurice, M. S., "An Investigation of Laser Velocimetry Particle Behavior within Flow Structures at Mach 12," AIAA Paper 94-0668, Jan. 1994.

[2]Molten, R. G., "Results from a Flowfield Survey of the Air Force Wright Aeronautical Laboratory Twenty Inch Hypersonic Wind Tunnel," Air Force Wright Aeronautical Lab., AFWAL-TM-88-187-FIMG, Wright Patterson AFB, OH, Sept. 1988.

[3]Ames Research Staff, "Equations, Tables and Charts for Compressible Flow," NACA Report 1135, 1953.

[4]Keyes, F. G., "A Summary of Viscosity and Heat Conduction Data for He, Ar, H_2, O_2, N_2, CO, CO_2, H_2O, and Air," *Transactions of the American Society of Mechanical Engineers*, Vol. 73, July 1951, pp. 589–596.

[5]Trolier, J. W., "Hypersonic Nozzle Flow Simulation Task 3," Science Applications International Corporation, SAIC/VF-88:004, Wayne, PA, Dec. 1988.

[6]Maurice, M. S., "Quantitative Laser Velocimetry Measurements in the Hypersonic Regime by the Integration of Experimental and Computational Analysis," AIAA Paper 93-0089, Jan. 1993.

Calculation of Wing-Alone Aerodynamics to High Angles of Attack

F. G. Moore* and R. M. McInville†
Naval Surface Warfare Center, Dahlgren, Virginia 22448-5100

Introduction

THE recent version of the NSWCDD Aeroprediction Code (AP93) released to the public[1–3] was limited in angle of attack (AOA) to about 30 deg because the wing-alone, wing-body, and body-wing interference aerodynamics were developed only up to about 30-deg AOA. In some cases, the accuracy degraded at an AOA of 25 deg. One reason for this degradation was the second-order accuracy of the method derived for the wing-alone solution. While this method gave much better estimates of wing aerodynamics than the linear theory of the 1981 version of the Aeroprediction Code (AP81) above α of about 10 deg, it still failed for AOA greater than about 30 deg.

To understand why the second order method fails at $\alpha \geq 30$ deg, refer to Fig. 1. Figure 1 examines the physical characteristics of the wing-alone normal force C_{Nw} and normal-force coefficient derivative $C_{N\alpha}$ as a function of aspect ratio (AR) and Mach number (M_∞). As seen in Fig. 1, at low to moderate values of the AR, typical

Received April 1, 1994; revision received Sept. 9, 1994; accepted for publication Sept. 12, 1994. This paper is declared a work of the U.S. Government and is not subject to copyright protection in the United States.

*Senior Aerodynamicist, Code G04, Weapons Systems Department, Dahlgren Division, 17320 Dahlgren Road. Associate Fellow AIAA.

†Aerospace Engineer, Code G23, Aeromechanics Branch, Dahlgren Division, 17320 Dahlgren Road.